Three-dimensional bi-functional lens based on conformal mapping

Jian Tang and Wei Xiang Jiang
State Key Laboratory of Millimeter Waves, Department of Radio Engineering, Southeast University
Nanjing 210096, China
E-mail: wxjiang81@seu.edu.cn

***Abstract*—In this work, we present a hemi-ellipsoidal bi-functional lens based on the technique of conformal mapping. When the feed is placed between two foci, the lens can be considered as a deflecting lens, which guides the waves to propagate to a deflecting angle; when the feed is placed on the long axis but outside the foci, the waves are guided along a U-shaped path and the lens can be considered as a U-shaped waveguide bend. We first design such a bi-functional lens based on conformal mapping and then rotate the lens around the central axis, hence we obtain a three-dimensional bi-functional lens. Ray tracing and full-wave simulation results verify the performance of the designed lens.**

***Keywords*—conformal mapping; ray tracing; three-dimensional lens; bi-functional lens.**

I. INTRODUCTION

Conformal mapping, as a special case of spatial transformation, has provided a powerful tool to design inhomogeneous but isotropic electromagnetic devices. The technique is based on form invariance of Maxwell's equations under spatial coordinate transformation [1-6]. The most representative work on conformal mapping is the so-called invisible cloaks [1] and other novel devices have also been proposed and designed, such as, bend waveguides[7-9], cylindrical-to-plane-wave conversion lens[10], and so on [11-13].

In this paper, we design a hemi-ellipsoidal bi-functional lens using conformal mapping, and verify the lens performance by ray-tracing and full-wave simulations. When the feed is placed between two foci, the lens can be considered as a deflecting lens, which guides the waves to propagate to a deflecting angle; when the feed is placed on the long axis but outside the foci, the waves are guided along a U-shaped path and the lens can be considered as a U-shaped waveguide bend. We first design such a bi-functional lens based on conformal mapping and then rotate the lens around the central axis, hence we obtain a three-dimensional bi-functional lens.

II. DESIGN AND NUMERICAL SIMULATION

The conformal mapping we consider here is the complex function $\cosh$, which transforms the complex plane $z = x + iy$ into another one $w = u + iv$. Then we have,

$$w = c * \cosh z = c * \cosh x * \cos y + c * \sinh x * \sin y \, , \tag{1}$$

where c is the focal length of the elliptic curve. For this conformal mapping, two sets of orthogonal curves are expressed as,

$$\begin{cases} \dfrac{u^2}{c^2 * \cosh^2 y} + \dfrac{u^2}{c^2 * \sinh^2 y} = 1 \\ \dfrac{u^2}{c^2 \cos^2 x} + \dfrac{v^2}{c^2 * \sin^2 x} = 1 \end{cases} . \tag{2}$$

The schematic diagram of the virtual and physical spaces is shown in Fig. 1. In the virtual space, the material is homogeneous and the waves will propagate along the straight lines. The material parameters in the physical space can be calculated as follows [1],

$$n = n_0 \Big/ \left| \frac{dw}{dz} \right| , \tag{3}$$

where n_0 indicates the refraction index in the virtual space. Here, we assume that the virtual space is free space with $n_0 = 1$, and then

$$n = \frac{1}{\left[\left(1 - \left(\frac{u}{c}\right)^2 + \left(\frac{v}{c}\right)^2 \right)^2 + 4 * \left(\frac{u}{c}\right)^2 * \left(\frac{v}{c}\right)^2 \right]^{1/4}} . \tag{4}$$

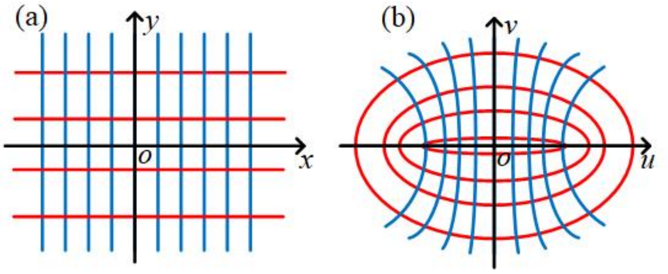

Fig. 1. Illustration of the conformal mapping between virtual and physical spaces. (a) The virtual space with a simple and homogeneous medium. (b) The physical space with transformed medium.

The intersecting angles of the orthogonal curves remain unchanged under conformal mapping. As illustrated in the Fig. 1, the vertical blue lines in Fig. 1(a) are mapped to the blue hyperbolic curves in Fig. 1(b), while the horizontal red lines are transformed into red elliptical curves. We use the conformal mapping described here to design a bi-functional lens by moving the feed location along the long *U* axis. We choose the long semi-axis *a*=75 mm and short semi-axis *b*=65mm. We calculate the refraction index of the hemi-elliptic lens by using Eq. (4) and the result is shown in Fig. 2(a).

To verify the functions of the semi-elliptic lens, we make some ray-tracing simulations and the working frequency is chosen as 18GHz. The ray-tracing results are shown in Figs. 2(b-d). When the feeding source is placed at the center of the ellipse, the rays propagate through the lens directly and then radiate to the space, as shown in Fig. 2(b); when we move the feeding source near the focal point, the rays will be deflected and then radiate to the free space in Fig. 2(c). However, when we continue to move the feeding source to the outside of the focal point and near the boundary of the ellipse, the rays are guided to propagate along the U-shaped path and the lens can be considered as a bend waveguide.

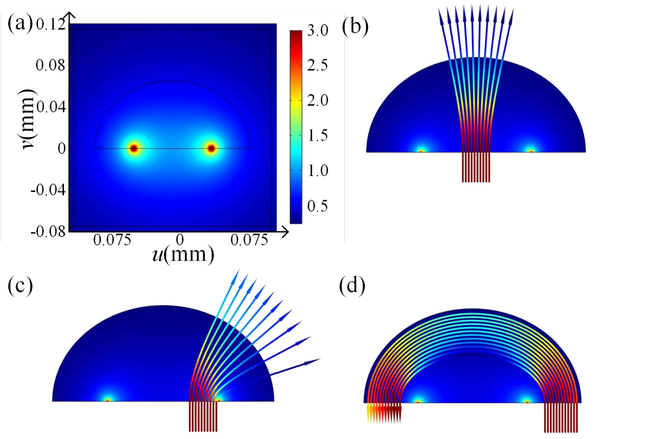

Fig. 2. (a) The refraction index distribution of the transformed lens. The ray-tracing results: (b) when the feeding source is at the center of the hemi-elliptic lens, (c) when the feeding source is near the focal point of the hemi-elliptic lens from the inside, (d) when the feeding source is near the inner boundary of the hemi-elliptic lens.

To further validate the performance of the designed bi-functional lens, we also make the full-wave simulations, and the results are shown in Fig. 3. Again, we observe that, when the feed is placed between two foci, the lens will guide the waves to propagate to a deflecting angle, as shown in Figs. 3(a-c); when the feed is placed on the long axis but outside the foci, the waves are guided along a U-shaped path, as shown in Fig. 3(d).

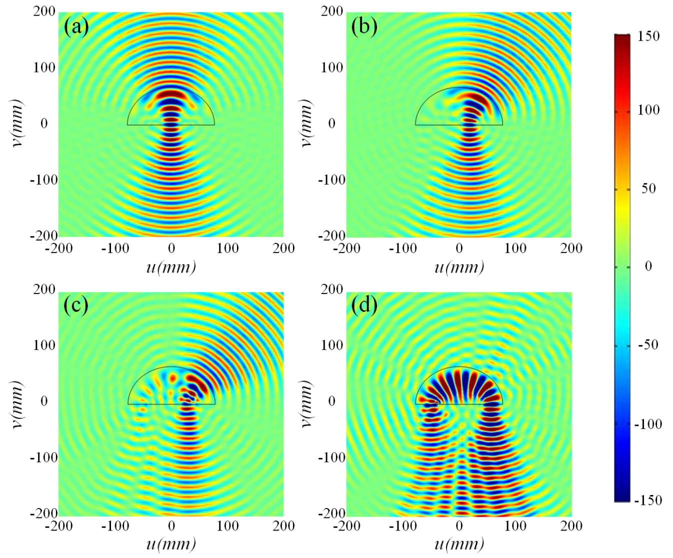

Fig. 3. Simulated electric-field distributions of the bi-functional lens at 18 GHz when the distances between the center of the focal points of hemi-elliptical lens and the feeding source are different. (a) the distance *u*=0 mm; (b) the distance *u*=18 mm; (c) the distance *u*=28 mm; (d) the distance *u*=52 mm.

III. Three-dimensinoal Bi-functional Lens

All we discussed above is a two-dimensional (2D) lens. Here, we extend the lens to a three-dimensional (3D) one by rotating the 2D lens along the center axis, in such a case, the refraction index can be expressed as,

$$n=\frac{1}{\left[\left(1-\left(\frac{u}{c}\right)^2-\left(\frac{w}{c}\right)^2+\left(\frac{v}{c}\right)^2\right)^2+4*\left(\left(\frac{u}{c}\right)^2+\left(\frac{w}{c}\right)^2\right)*\left(\frac{v}{c}\right)^2\right]^{1/4}} \tag{5}$$

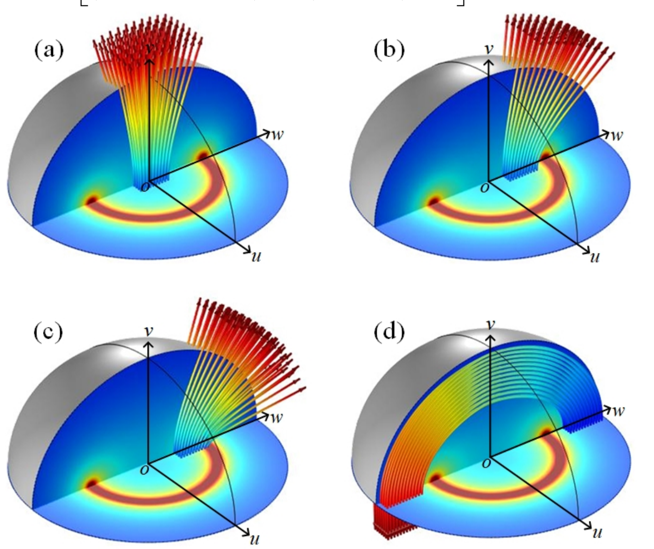

Fig. 4. The ray-tracing results of the 3D bi-functional lens when the distances between the center of excitation plane of hemi-ellipsoidal lens and the feeding source are different. (a) the distance *u*=0 mm; (b) the distance *u*=18 mm; (c) the distance *u*=28 mm; (d) the distance *u*=52 mm.

To illustrate the performances of the 3D transformation-optics bi-functional lens, we simulate electromagnetic wave propagation by using ray tracing. The simulation results are demonstrated in Fig. 4. When the feed is located at the center of the bottom of the 3D lens, the ray-tracing results of the propagation path are shown in Fig. 4(a). As we gradually move feed away from the center point to the focal circle, the waves will start to deflect and deflection angle increases gradually. When we place the feed between the focal circle and the boundary of the lens, the rays will propagate along the U-shaped path, as illustrated in Fig. 4(d). In such as case, the 3D lens acts as a bend waveguide.

IV. CONCLUSIONS

Based on conformal mapping, we present a three-dimensional bi-functional lens and the performance is verified by simulation results. When the feeding source is placed inside the focal circle at the bottom plane of the lens, rays will deflect to different directions and the lens acts a deflection lens; when the feeding source is placed between the focal circle and the boundary of the lens, rays will be guided along U-shaped path and the lens acts bend waveguide. The presented bi-functional lens can also be extended to other wave dynamics, such as, acoustics wave.

ACKNOWLEDGMENT

This work was supported by the National Science Foundation of China (61522106, 61571117, 61501112, 61401089, 61501117, 61631007, and 61731010), the Foundation of National Excellent Doctoral Dissertation of China (201444), and the 111 Project (111-2-05).

REFERENCES

[1] U. Leonhardt, "Optical conformal mapping," Science 312(5781), 1777-1780 (2006).

[2] J.B. Pendry, D. Schuring, and D.R. Smith, "Controlling electromagnetic field," Science 312(5781), 1780-1782 (2006).

[3] S. Ramo, J.R. Whinnery, and T. Van Duzer, Fields and Waves in Communication Electronics (3rd edn), Ch. 7 (Wiley, 1994).

[4] M. Lax, and D.F. Nelson, "Maxwell equations in material form," Phys. Rev. B 13(4), 1777-1784 (1976).

[5] D. Schurig, J.B. Pendry, and D.R. Smith, "Calculation of material properties and ray tracing in transformation media," Opt. Express 14(21), 9794-9804 (2006).

[6] U. Leonhardt, and T.G. Philbin, "General relativity in electrical engineering," New J. Phys. 8, 247 (2006).

[7] M.L. Wu, P.L. Fan, J.M. Hsu, and C.T. Lee, "Design of ideal structures for lossless bends in optical waveguides by conformal mapping," IEEE J. Lightw. Technol. 14(11), 2604-2614 (1996).

[8] Y.G. Ma, N. Wang, and C.K. Ong, "Application of inverse, strict conformal transformation to design waveguide devices," J. Opt. Soc. Am. A 27(5), 968-972 (2010).

[9] K. Yao and X. Jiang, "Designing feasible optical devices via conformal mapping," J. Opt. Soc. Am. B 28(5), 1037-1042 (2011).

[10] W.X. Jiang, "Cylindrical-to-plane-wave conversion via embedded optical transformation." Applied Physics Letters 92(26): 261903(2008).

[11] H.Y. Chen, Y.D. Xu, H.Li, and T. Tyc, "Playing the tricks of numbers of light sources," New J. Phys 15(9), 093034 (2013).

[12] J.P. Turpin, A.T. Massoud, Z.H. Jiang, P.L. Werner, and D.H. Werner, "Conformal mappings to achieve simple material parameters for transformation optics devices," Opt. Express 18(1), 244-252 (2010).

[13] C. Lu, and Z.L. Mei, "Multi-functional lens based on conformal mapping," Opt. Express 23(15), 19901-19910(2015).